Al-Qadisiyah Journal of Pure Science

Volume 29 | Number 2 Article 15

12-20-2024

Effect of Ag Doped Nanostructure CuO Thin Films

Q.S. Kareem
Department of Physics, University of Qadisiya, College of Education, Iraq, qasim.alshook@qu.edu.iq

ORIGINAL STUDY

Effect of Ag Doped Nanostructure CuO Thin Films

Qasim Sattar Kareem

Department of Physics, University of Qadisiya, College of Education, Iraq

Abstract

In this experiment, the nanoparticles Bimetallic NPCuOAg was already made using the chemical spray pyrolysis process. Shap and structure CuOAg nanosheets was tested via XRD & AFM was investigated. XRD shown impacted of Ag doping from (0−4) % reason decreasing crystallite size, as microstrain and dislocation density are increasing. Also, AFM analysis of NPCuOAg a hierarchical structure where CuO thin films are regularly established with three dimensional nanoparticles Ag skeleton. The optical characteristics confirm that when Ag doping increases, the energy gap reduces from (2.4−2.32) eV.

Keywords: CuOAg thin films, Particle size, Doping, Nanoparticles bimetallic

1. Introduction

Nano-particular materials have many of characteristics. They have been utilized in catalysis, sensors and more [1−17]. Making nano - size metals using the CAPM way was one of the successful methods [16]. Due to its broad applications in wide ranges, trhe thin films, nanorods and powder were made via (ZnO and CuO) has been vast research [18,19]. In this study, the production of a bimetallic NPCuAg by (CSPM) is taken into account in order to examine the structure, thermal treatment, and morphology of CuOAg.

2. Experimental

By use of the chemical spray pyrolysis process, thin films of CuO were made. Taking 0.1 M copper chloride (CuCl2.2H2O) dissolved in 100 mL de - ionized water, these films were applied to clean plate surfaces. In the percentage range of 2−4, AgNo3 was utilized as a doping material. The temperature of the substrate was maintained during 300 °C, 2 percentages were supplied to the matrix liquid after the matrix liquid had been deposited to produce (2 & 4) % Ag dopants. The following preparatory requirements were established. The substrate was kept as 350 °C for the length of the deposition stage. Carrier gas used was nitrogen, The gap between the substrate and the nozzle was 27 c_m Spritzing period, rate, and the gap among two spraying methods were all 10 s, 5 mL per minute, and 2 min, respectively. Using a UVvisible double beam spectrophotometer, the transmittance, and absorbance spectra were acquired in 400−900 nm wavelength.

3. Result and discussion

3.1. Structural studies

Fig. 1 appear XRD of CuO at several Ag doping via (CSPM). In polycrystalline hexagonal, CuO films do occur at 0 % [20]. When 2 % Ag doping was used to improve peak intensity peaks at the reflection, The crystal plane of the initial nuclei may continue to be parallel to the film surface despite the fact that rising in Ag reduces the amount of crystallinity of thin film as a result of the film rising of initial nuclei, since the crystal level, with the lowest surface free energy grows more slowly than the other crystal level. It is important to note Ag doping of 4 % marked the transition from the hexagonal structure to the cube at the reflection 110 as the angle 2θ is 33.05° as indicated in lower images connected Fig. 1. There were many secondary reflections, at (110), at 2θ equal to 32.98°, 32.98° and 33.05, chemical spray pyrolysis of CuO thin films revealed a phase

Received 23 May 2022; accepted 17 October 2022.

Available online 18 April 2025
E-mail address: qasim.alshook@qu.edu.iq.

https://doi.org/10.29350/2411-3514.1294

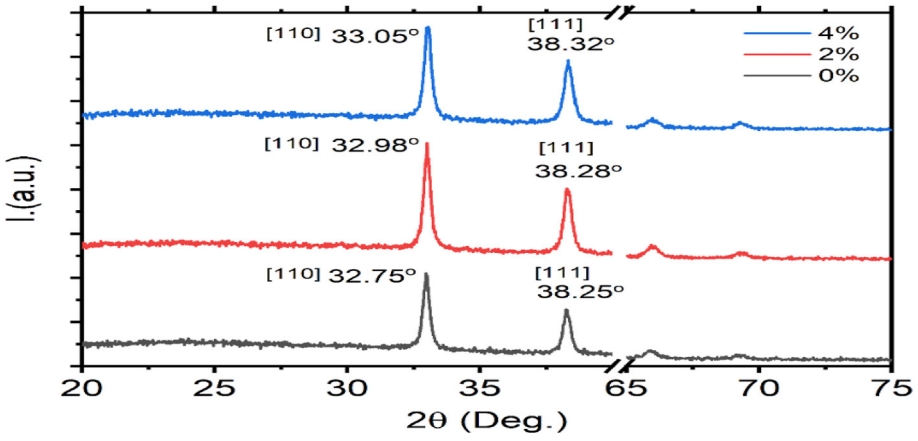

Fig. 1. XRD pattern of CuO at different Ag doping as (CSPM).

transition from hexagonal to cubic. The crystallite sizes via the XRD were calculated using standard (110) reflection at 2θ is 32.98°. As seen, increased Ag doping results in an acute increase in Bragg reflections, which allows for the detection of a decline in film crystallinity. Via Scherrer's equation, the crystallite size (D) was calculated [21].

$$D = \frac{k\lambda}{\beta \cos\theta} \tag{1}$$

Here K is the form factor, with a value of 0.9, θ the Bragg angle, β is the total width at half maximum and λ is the XRD wavelength. The equations were used to determine the lattice parameter amounts [21].

$$a = d\left(h^2 + k^2 + l^2\right)^{1/2} \tag{2}$$

$$\frac{1}{d^2} = \frac{4}{3}\frac{\left(h^2 + hk + k^2\right)}{a^2} + \frac{l^2}{c^2} \tag{3}$$

CuO thin films' crystallite size was 27.94 nm, and as Ag doping increased up to 4 %, it reduced to 27.69 nm. The number of crystallites per unit surface area can also be determined using this information to get the dislocation density. Equation (4), which depicts a lattice expansion or pressure, was used to measure microstrain (ε). Dislocation density (δ) was evaluated via equation (5). Table 1 represent the values of dislocation density and microstrain.

$$\varepsilon = \frac{\beta \cos\theta}{4} \tag{4}$$

Also, the films' tension was based on [17]:

$$\delta = \frac{1}{D^2} \tag{5}$$

3.2. Optical properties

Fig. 2(a) displays the transmittance curves for various deposition periods. The deposited films were transparent at average transmittance 55 %; however, as the Ag% doping rises, transmittance drops, and this is because film thickness rises. The measurements of the absorption coefficient (α) in Fig. 2(b) are, inversely proportional with Fig. 2(a). Optical energy gap (Eg) can be evaluated using equation (6). Fig. 2(c) displays curve of $(\alpha h\nu)^2$as photon energy (hν) [22].

$$(\alpha h\nu) = A\left(h\nu - \mathrm{E}_g\right)^n \tag{6}$$

n is a constant, ; it takes values of 1/2, for direct allowed. It is found that as the Ag doping % is increased, the Eg values of the CuOAg nanosheets

Table 1. Structural data of CuO at different Ag doping as (CSPM).

Ag Doping %	(hkl) Plane	2theta (Deg.)	Lattice constant (Å)		FWHM (Deg.)	Crystallite size D (nm)	Microstrain (line^{-2}.m^{-1}) × 10^{-3}	Dislocation density (δ) (line.m^{-2}) × 10^{15}
0	(110)	32.98	a 4.68	c 5.13	0.39	27.94	1.046	12.80
2	(110)	32.98	a 4.68	c 5.13	0.38	27.75	1.050	12.98
4	(110)	33.05	a 3.42		0.40	27.69	1.052	13.04

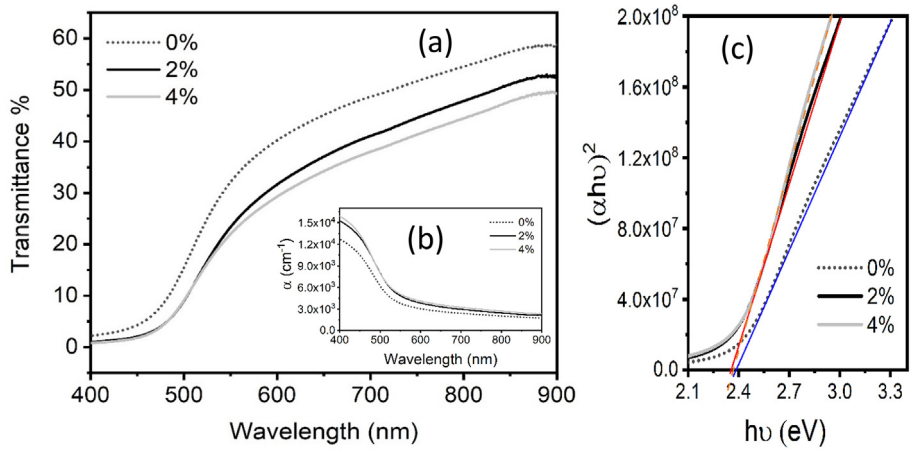

Fig. 2. (a) Tra. as λ for CuO at unlike Ag doping via (CSPM), (b) absorption coefficient (c) band gap.

reduce, leading to a decline in crystal size, a variation in film thickness, and it might be caused by quantum confinement [23]. Fig. 2(b) illustrates the values of the (α), which explains why the (Eg) type is direct. In Fig. 2(c), the Eg value is determined by extrapolating the straight line of the plot of $(\alpha h\nu)^2$ versus (hν), Along with their reliance in drawing the link amidst quantities of $(\alpha h\nu)^2$ and (hν), which are observed to decrease as the Ag% doping rises.

3.3. Atomic force microscopy

AFM pictures showed the surface structure of the thin films. Fig. 3 depicts a gradual rise in columnar

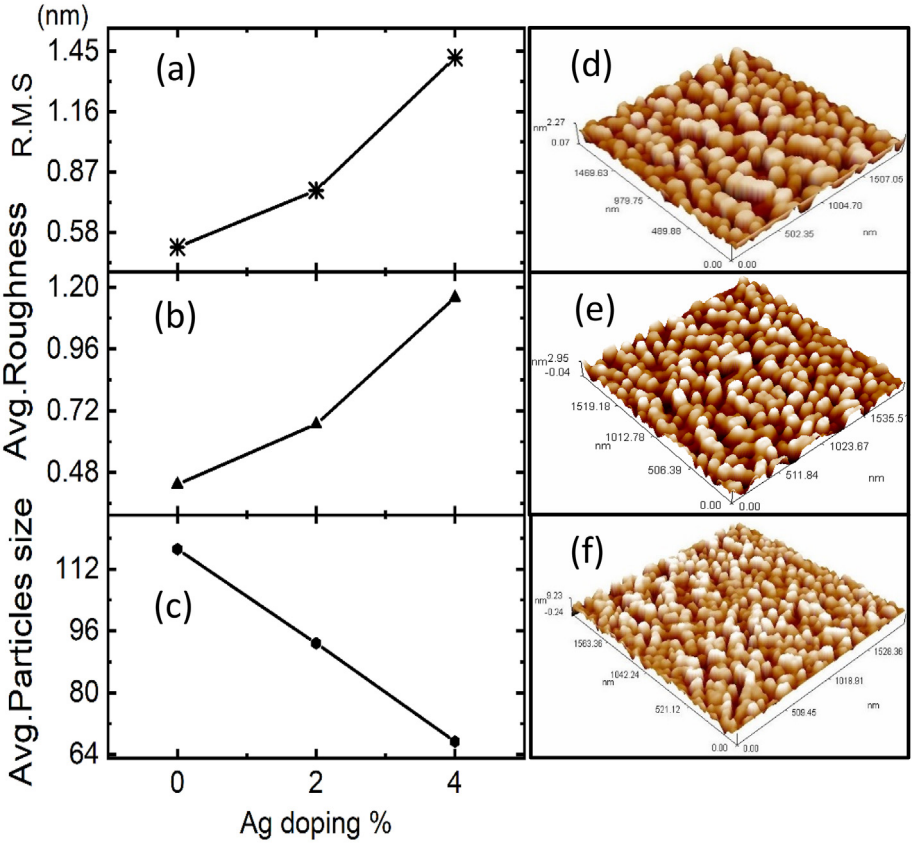

Fig. 3. AFM, 3D picture of CuOAg Nano-films (a, b and c) RMS, Roughness Average and Avg. Diameter, AFM pictures of CuOAg with % depositions of (d) 0 %, (e) 2 % and (c) 4 %.

size, surface area, and roughness. The growth might be impacted by the thickness and deposition period. According to Fig. (3a, b, and c), there a drop in average of average particle size at rises Ag dopants, which is accompanied by an increase in RMS and average roughness. The average roughness (Ra), root mean square (R.M.S.), time coating, and surface area all rise with Ag% doping. With Ag% doping, however, average particle size decreases. The rises in surface area is crucial for photocatalytic activity [24].

4. Conclusions

CuOAg Nano-films are made using various Ag dopants, At 0 % CuOAg, it is evident that films are polycrystalline and hexagonal, and 4 %, a fairly straightforward transition begins. Nano-films enter the hexagonal phase, resulting in smaller particles and better crystallization. The model for the measurement of the quantum confinement was the reduced particle to nano size with increasing Ag % doping.

Funding

This research received no specific grant from any funding agency in the public or commercial.

References

[1] Erlebacher J, Aziz MJ, Karma A, Dimitrov N, Sieradzki K. Nature 2001;410:450.
[2] Ding Y, Chen M. MRS Bull 2011;34:569.
[3] Snyder J, Fujita T, Chen MW, Erlebacher J. Nat Mater 2010;9:904.
[4] Qiu H, Dong X, Huang X. Nanoscale 2012;4:4492.
[5] Zhang J, Li CM. Chem Soc Rev 2012;41:7016.
[6] Lang X, Hirata A, Fujita T, Chen M. Nat Nano 2011;6:232.
[7] Ding Y, Zhang Z. In: Nanoporous metals for advanced energy technologies. Cham: Springer International Publishing; 2016. p. 175.
[8] Li R, Liu XJ, Wang H, Zhou DQ, Wu Y, Lu ZP. Acta Mater 2016;105:367.
[9] Yun Q, He Y-B, Lv W, Zhao Y, Li B, Kang F, et al. Adv Mater 2016;28:6932.
[10] C. Zhang, B. Huang, L. Qian, S. Yuan, S. Wang, and R. Chen, ChemPhysChem 2016;17:98–104
[11] Li R, Liu XJ, Wang H, Zhou DQ, Wu Y, Lu ZP. Acta Mater 2016;105:367.
[12] Qiu HJ, Kang JL, Liu P, Hirata A, Fujita T, Chen MW. J Power Sources 2014;247:896.
[13] Zeng Z, Long X, Zhou H, Guo E, Wang X, Hu Z. Electrochim Acta 2015;163:107.
[14] Hou Y, Chen L, Zhang L, Kang J, Fujita T, Jiang J, et al. J Power Sources 2013;225:304.
[15] Kang J, Hirata A, Qiu HJ, Chen L, Ge X, Fujita T, et al. Adv Mater 2014;26:269.
[16] Zhang J, Chan LC, Gao T, Wang Q, Zeng S, Bian H, et al. J Mater Chem A 2016;4:15057.
[17] Wang Z, Liu J, Qin C, Liu L, Zhao W, Inoue A. Intermetallics 2015;56:48. 17, 98 (2016).
[18] Chowa L, Lupana O, Chaia G, Khallafa H, Onoa LK, Cuenyaa BR, et al. Synthesis and characterization of Cu-doped ZnO one-dimensional structures for miniaturized sensor applications with faster response. Sens Actuators A Phys 2013;189:399–408.
[19] Li R, Wu N, Liu J, Jin Y, Chen X-B, Zhang T. Corrosion Sci 2017;119:23.
[20] Hsu Chih-Hung, Lung-Chien Chen, Xiuyu Zhang. Effect of the Cu source on optical properties of CuZnO films deposited by ultrasonic spraying. Materials (Basel, Switzerland) 2014;7(2):1261–1270. 18 Feb.
[21] Monshi Ahmad, Foroughi Mohammad Reza, Reza Monshi Mohammad. Modified scherrer equation to estimate more accurately nano-crystallite size using XRD. World J Nano Sci Eng 2012;2:154–60.
[22] Chiad SS, Jabbar WA, Habubi NF. Effects of annealing on the electronic transitions of ZnS thin films. Journal of the Arkansas Academy of Science 2011;65:39–42.
[23] Malliga P, Pandiarajan J, Prithivikumaran N, Neyvasagam K. Effect of film thickness on structural and optical properties of TiO2 thin films, IEEE Xplore, Proc. IEEE Conf. On advanced nano materials & emerging engineering technologies, Chennai, India. 2013. p. 547–50.
[24] Wold A. Photocatalytic properties of titanium dioxide (TiO_2). Chem Mater 1993;5(3):280–3.